RESEARCH ARTICLE

Human Mutation

OFFICIAL JOURNAL
HGVS
HUMAN GENOME VARIATION SOCIETY
www.hgvs.org

Mutations in *CCDC39* and *CCDC40* are the Major Cause of Primary Ciliary Dyskinesia with Axonemal Disorganization and Absent Inner Dynein Arms

Dinu Antony,[1†§] Anita Becker-Heck,[2‡§] Maimoona A. Zariwala,[3§] Miriam Schmidts,[1] Alexandros Onoufriadis,[1] Mitra Forouhan,[1] Robert Wilson,[4] Theresa Taylor-Cox,[5] Ann Dewar,[5] Claire Jackson,[6] Patricia Goggin,[6] Niki T. Loges,[2] Heike Olbrich,[2] Martine Jaspers,[7] Mark Jorissen,[7] Margaret W. Leigh,[8] Whitney E. Wolf,[9] M. Leigh Anne Daniels,[9] Peadar G. Noone,[9] Thomas W. Ferkol,[10] Scott D. Sagel,[11] Margaret Rosenfeld,[12] Andrew Rutman,[13] Abhijit Dixit,[14] Christopher O'Callaghan,[13] Jane S. Lucas,[6] Claire Hogg,[5] Peter J. Scambler,[1] Richard D. Emes,[15] UK10K,[16] Eddie M.K. Chung,[17] Amelia Shoemark,[5] Michael R. Knowles,[9*§] Heymut Omran,[2*§] and Hannah M. Mitchison[1*§]

[1]Molecular Medicine Unit and Birth Defects Research Centre, University College London (UCL) Institute of Child Health, London, UK; [2]Department of Pediatrics and Adolescent Medicine, University Hospital Muenster, Muenster, Germany; [3]Department of Pathology and Laboratory Medicine, UNC School of Medicine, Chapel Hill, North Carolina; [4]Respiratory Medicine, Royal Brompton and Harefield NHS Trust, London, UK; [5]Department of Paediatric Respiratory Medicine and Electron Microscopy Unit, Royal Brompton and Harefield NHS Trust, London, UK; [6]Primary Ciliary Dyskinesia Group, University of Southampton Faculty of Medicine, Southampton NIHR Respiratory Biomedical Research Unit, Southampton General Hospital, Southampton, UK; [7]University Hospitals Leuven, Department of Otorhinolaryngology, Leuven, Belgium; [8]Department of Pediatrics, UNC School of Medicine, Chapel Hill, North Carolina; [9]Department of Medicine, UNC School of Medicine, Chapel Hill, North Carolina; [10]Department of Pediatrics, Washington University School of Medicine, St. Louis, Missouri; [11]Department of Pediatrics, University of Colorado School of Medicine, Aurora, Colorado; [12]Children's Hospital and Regional Medical Center, Seattle, Washington; [13]Department of Infection, Immunity and Inflammation, University of Leicester, Leicester Royal Infirmary, Leicester, UK; [14]Department of Clinical Genetics, Nottingham City Hospital, Nottingham, UK; [15]School of Veterinary Medicine and Science, University of Nottingham, Leicestershire, UK; [16]uk10k.org.uk; [17]General and Adolescent Paediatric Unit, University College London (UCL) Institute of Child Health, London, UK

Communicated by Ravi Savarirayan

Received 14 June 2012; accepted revised manuscript 19 November 2012.
Published online 15 December 2012 in Wiley Online Library (www.wiley.com/humanmutation). DOI: 10.1002/humu.22261

ABSTRACT: Primary ciliary dyskinesia (PCD) is a genetically heterogeneous disorder caused by cilia and sperm dysmotility. About 12% of cases show perturbed 9+2 microtubule cilia structure and inner dynein arm (IDA) loss, historically termed "radial spoke defect." We sequenced CCDC39 and CCDC40 in 54 "radial spoke defect" families, as these are the two genes identified so far to cause this defect. We discovered biallelic mutations in a remarkable 69% (37/54) of families, including identification of 25 (19 novel) mutant alleles (12 in CCDC39 and 13 in CCDC40). All the mutations were nonsense, splice, and frameshift predicting early protein truncation, which suggests this defect is caused by "null" alleles conferring complete protein loss. Most families (73%; 27/37) had homozygous mutations, including families from outbred populations. A major putative hotspot mutation was identified, CCDC40 c.248delC, as well as several other possible hotspot mutations. Together, these findings highlight the key role of CCDC39 and CCDC40 in PCD with axonemal disorganization and IDA loss, and these genes represent major candidates for genetic testing in families affected by this ciliary phenotype. We show that radial spoke structures are largely intact in these patients and propose this ciliary ultrastructural abnormality be referred to as "IDA and microtubular disorganisation defect," rather than "radial spoke defect."

Hum Mutat 00:1–11, 2013. © 2012 Wiley Periodicals, Inc.

KEY WORDS: primary ciliary dyskinesia; cilia; CCDC39; CCDC40; radial spoke; dynein regulatory complex; nexin link

Additional Supporting Information may be found in the online version of this article.

†Present address: Dasman Genome Center Unit, P.O.Box 1180, Dasman 15462, Kuwait.

‡Present address: Developmental and Molecular Pathways, Novartis Institutes for BioMedical Research, Forum 1, Novartis Campus Basel, CH-4056, Basel, Switzerland.

§These authors contributed equally to this work.

*Correspondence to: Hannah M. Mitchison, Molecular Genetics Unit and Birth Defects Research Centre, University College London (UCL) Institute of Child Health, 30 Guilford Street, London WC1N 1EH, UK; E-mail: h.mitchison@ucl.ac.uk or Heymut Omran, Department of Pediatrics and Adolescent Medicine, University Hospital Muenster, Muenster, Germany; E-mail: heymut.omran@ukmuenster.de or Michael R. Knowles, Department of Medicine; UNC School of Medicine, Chapel Hill, NC; E-mail. knowles@med.unc.edu

Contract grant sponsors: Wellcome Trust (WT091310); National Institute of Health (5 U54 HL096458–06, 5 R01HL071798); National Center of Research Resources (ULI TR000083, 5 U54 HL096458–06, UL1 TR000154); Kindness for Kids Foundation; European Community (SYS-CILIA); Schröder-Stiftung; Action Medical Research and Newlife Foundation; The Henry Smith Charity.

Introduction

Primary ciliary dyskinesia (PCD) is a recessively inherited disorder, which arises from cilia/sperm dysmotility that is associated with a number of different axonemal ultrastructural abnormalities. The symptoms of deficient mucociliary clearance are usually obvious from birth, and patients have recurrent respiratory tract infections leading to irreversible lung damage (bronchiectasis). They also manifest with otitis media, chronic sinusitis, and subfertility. Internal organ laterality is randomized with about half of patients having situs inversus, an association reflecting dysmotility of nodal cilia during embryonic development.

Motile flagella and cilia are related organelles found on the surface of cells evolutionarily conserved across 1.6 billion years from the flagella of the green alga *Chlamydomonas* to the ciliated respiratory and embryonic node cells of vertebrates [Pazour, 2004]. In humans, motile cilia have a common microtubule-based ultrastructure (axoneme), comprising nine peripheral microtubule doublets either surrounding (in "9+2" motile respiratory and fallopian tube cilia, and sperm flagella) or lacking (in "9+0" motile nodal cilia) a central microtubule pair [Becker-Heck et al., 2012; Fliegauf et al., 2007], and linked to a variety of microtubule-associated proteins. These include the inner and outer dynein arm (IDA and ODA) motor complexes, which project from the peripheral microtubule doublets; the radial spokes, which provide a radial scaffold between the central pair and peripheral microtubules and facilitate signal transduction from the center out to the dynein arms to govern ciliary beat and waveform [Becker-Heck et al., 2012]; and nexin–dynein regulatory complexes (N-DRC), which attach between adjacent peripheral doublets to facilitate IDA attachment and regulate dynein activity [Heuser et al., 2009]. This complex superstructure creates the rigid organization along the entire length of the axoneme, which is required for motor ATPase signaling to generate a uniquely coordinated and self-propagating beat [Mitchison and Mitchison, 2010].

PCD is genetically heterogeneous with 18 identified genes causing nonsyndromic disease. The large range of genetic defects cause a small number of defective ciliary ultrastructural subtypes according to current imaging resolution, and no correlations have been defined between ultrastructural defects and the course of disease [Kispert et al., 2003]. Mutations in genes that cause axonemal ODA defects (*DNAH5*, *DNAI1*, *DNAI2*, *DNAL1*, *TXNDC3*, and *CCDC114*) are the genetic basis of the majority of PCD cases [Bartoloni et al., 2002; Duriez et al., 2007; Knowles et al., 2012; Loges et al., 2008; Mazor et al., 2011; Olbrich et al., 2002; Onoufriadis et al., in press; Pennarun et al., 1999]. Mutations in genes encoding components of the radial spoke head (*RSPH4A* and *RSPH9*) cause defects involving the central pair microtubules [Castleman et al., 2009]. Mutations in genes encoding cytoplasmic or dual location proteins with putative roles in the assembly and transport of dynein arm components from the cell body and their localization to the axoneme (*DNAAF1/LRRC50*, *DNAAF2/KTU*, *DNAAF3/PF22*, *CCDC103*, *HEATR2*, and *LRRC6*) cause IDA and ODA defects [Duquesnoy et al., 2009; Horani et al., 2012; Kott et al., 2012; Loges et al., 2009; Mitchison et al., 2012; Omran et al., 2008; Panizzi et al., 2012]. Two genes associated with PCD give rise to no discernible ultrastructural defects of the axoneme (*DNAH11*) or defects of the central microtubule pair C2b projection that are too subtle to be easily detected (*HYDIN)* [Bartoloni et al., 2002; Knowles et al., in press; Olbrich et al., 2012].

Lastly, mutations in two genes, *CCDC39* (MIM #613798) [Merveille et al., 2011] and *CCDC40* (MIM #613799) [Becker-Heck et al., 2011], have recently been shown in PCD patients that have a defect of the cilia axoneme, involving loss of the IDAs accompanied by a variably expressed disorganization of the 9+2 microtubule arrangement. Recent transmission electron microscopy (TEM) surveys of several different PCD cohorts estimated that at least ∼12% of all PCD cases have this defect [Chilvers et al., 2003; Papon et al., 2010; Shoemark et al., 2012]. The nine peripheral microtubules are retained but are mislocalized, often becoming more centralized, whereas the central microtubule pair may be variously lost (9+0), eccentrically positioned toward the periphery (9+2), or increased in number with a supernumerary central pair present (9+4); and the IDA structures are reduced or absent. Furthermore, in axonemes with this defect abnormal and/or absent N-DRC [Konradova et al., 1982; Schneeberger et al., 1980] and radial spokes [Antonelli et al., 1981; Sturgess et al., 1979] have been recorded. This ultrastructural defect has historically often been referred to as "radial spoke defect." The reasons for the various disarrangements are unclear, but because a range of microtubule disorganizations may be seen within a single TEM sample of respiratory epithelia from a patient, it is even possible that a variety of changes may occur along the length of the axoneme. These perturbations of structure create a characteristic ciliary motility defect with a beating pattern of mixed appearance, where stiff cilia displaying a reduced amplitude (70%) and cilia that are fully immotile (30%) are both visible [Becker-Heck et al., 2011; Chilvers et al., 2003; Merveille et al., 2011]. The partially retained motility may be explained by activity of the ODA motors, but cilia waveform is misregulated and the mean ciliary beat frequency (CBF) is reduced [Chilvers et al., 2003].

The *CCDC39* and *CCDC40* genes encode structurally related coiled-coil domain-containing proteins of unknown function that are localized to the axoneme [Becker-Heck et al., 2011; Merveille et al., 2011]. The loss of IDAs and N-DRC from ciliary axonemes of *CCDC39* and *CCDC40* patients has been previously confirmed using antibodies to DNALI1 and the N-DRC component GAS11/8, respectively [Becker-Heck et al., 2011; Merveille et al., 2011], and it is proposed that CCDC39 and CCDC40 proteins interact with N-DRC components and play a role in IDA attachment. Neither protein has yet been identified in proteomic studies of N-DRC composition [Lin et al., 2011]; thus, rather than being integral N-DRC proteins, they may be otherwise involved in N-DRC assembly, microtubule attachment, or protein interactions. The role of the CCDC39 and CCDC40 proteins in the structure and function of radial spokes is not known, and radial spokes in cilia from "radial spoke defect" patients have never been examined at the molecular level using antibody staining techniques.

In this study, we applied a combination of candidate gene Sanger sequencing and next-generation whole exome sequencing to identify the genetic cause of PCD in a large cohort of "radial spoke defect" patients with cilia dysmotility associated with axonemal microtubule disorganization and absence of IDAs. We also used antibody and immunofluorescence techniques to investigate radial spoke perturbations in nasal ciliated cells in patients with *CCDC39/40* mutations.

Materials and Methods

Subjects

A total of 54 unrelated PCD families were involved in the screen. Parallel mutational analysis on a collection of 17 families from UCL-ICH (labeled in the text by "UCL" prefix), four from Belgium/UHM (University Hospital Muenster) ("OP" and "KUL" prefix), and 33 from UNC ("UNC" prefix) was performed using genomic DNA samples obtained from peripheral blood cells. All families agreed under informed consent to participate in this study in accordance with protocols approved by the ethical committees of the Institute of

Child Health/Great Ormond Street Hospital and University College London Hospital NHS Trust, and those of collaborating institutions.

CCDC39 and *CCDC40* Mutation Identification

The transcripts referred to are *CCDC39* NM_181426.1 and *CCDC40* NM_017950.2. Sanger sequencing was performed by amplifying and sequencing the coding exons and flanking intronic sequences of *CCDC39* and *CCDC40* (primer sequence available on request). Sequence alignments for variant identification were made using Sequencher software (Gene Codes Corporation, Ann Arbor, MI, USA). Whole exome sequencing was performed for most samples by capturing the exons using the Agilent SureSelect All Exon Human V3 (50 Mb) kit (Agilent Technologies Ltd., Berkshire, UK). TruSeq Pair End Cluster kit V3 was used for cluster generation and 100 bp paired-end reads were generated on an Illumina HiSeq 2000 analyzer (Illumina Inc., Essex, UK) using Illumina TruSeq V3 SBS sequencing chemistry. The BWA alignment tool [Li and Durbin, 2010] was used to map sequence reads back to the genome (human reference hg19), then the GATK tool suite [McKenna et al., 2010] was used to process the alignments and identify variations. The SNP-Effects (http://snpeff.sourceforge.net/) and ANNOVAR [Wang et al., 2010] programs were used to annotate variations. The details of the whole exome sequencing are presented in Supp. Table S1.

In one case (PCD22) exome sequencing was performed as part of the Wellcome Trust Sanger Institute UK10K Project as described previously [Olbrich et al., 2012; Onoufriadis et al., in press]. Exome variant analysis was achieved by filtering of the total variant list according to consistent autosomal recessive inheritance pattern, novelty in comparison with human polymorphism databases including the 1000 Genomes (2010 1000 Genomes project Consortium, 2010) and NHLBI Exome Sequencing projects (http://evs.gs.washington.edu/EVS) and dbSNP v135 [Sherry et al., 2001], and finally for their functional significance. This analysis required the presence of at least one homozygous or two heterozygous changes occurring with an estimated frequency <0.01, and all the patients included in this study had clear-cut biallelic variants in the *CCDC39* and *CCDC40* genes that were identified via excellent coverage in all cases, without any other obvious causal candidates indicated. Sanger sequencing was used to confirm all the identified variants from exome sequencing and to verify the segregation pattern of each change in other unaffected family members, identified by both methods.

Nucleotide numbering reflects cDNA numbering with +1 corresponding to the A of the ATG translation initiation codon in the reference sequence, according to journal guidelines (www.hgvs.org/mutnomen). The initiation codon is codon 1.

Electron Microscopy and High-Speed Video Light Microscopy

Respiratory epithelial cells were obtained using a cytology brush or rhinoprobe from the inferior turbinate of participants and immediately analyzed for cilia beat frequency and beat pattern under light microscopy as described [Chilvers et al., 2003]. Samples were fixed in glutaraldehyde and an ultrastructural defect of the cilia was confirmed by electron microscopy [Rutland et al., 1982].

Immunofluorescence Analysis

The effect of the *CCDC40* splice mutation in patient UCL114 II:1 was confirmed by immunofluorescence analysis. Respiratory epithelial cells obtained by nasal brush biopsy were suspended in cell culture medium. Samples were spread onto glass slides, air dried and stored at −80°C until use. Cells were fixed with 4% PFA for 4 min at room temperature, washed 5× with PBS and then permeabilized with 0.5% Triton X-100 for 10 min. After five more washes with PBS cells were incubated with 5% bovine serum albumin (Sigma-Aldrich, Dorset, UK) in PBS for 1 hr. The cells were then incubated with primary antibodies overnight at room temperature using the following dilutions: CCDC39 antibody 1:100 (rabbit polyclonal; Sigma); RSPH4A 1:100 (rabbit polyclonal; Sigma); ROPN1L 1:200 (rabbit polyclonal; Sigma) monoclonal mouse antiacetylated and gamma tubulin 1:500 (Sigma) overnight at room temperature. After five washes with PBS cells were incubated with secondary antirabbit antibody (Alexa Fluor 488 Molecular Probes; Life Technologies, Paisley, UK) and secondary antimouse antibody (Alexa Fluor 594 Molecular Probes; Invitrogen). DNA was stained using DAPI (Life Technologies, Paisley, UK). Cells were finally washed 5× with PBS, mounted in Vectashield (Vector Laboratories Ltd., Peterborough, UK) and confocal images were taken using a Zeiss LSM 710 (Zeiss Ltd., Cambridge, UK).

Protein Modeling

Conserved domains were predicted using SMART [Letunic et al., 2012] and CDD [Marchler-Bauer et al., 2011], and coiled-coil protein folds predicted using Paircoil2 [McDonnell et al., 2006] with minimum window size of 28 amino acids. Protein homologies and network predictions were identified using PSI-BLAST [Altschul et al., 1997] to search the nr database and STRING 9.0 [Szklarczyk et al., 2011].

Results

The entire coding region and flanking intronic sequences of the *CCDC39* and *CCDC40* genes were sequenced in a cohort of 59 patients from 54 PCD families that displayed ciliary dysmotility and a similar axonemal ultrastructural phenotype to that associated with *CCDC39* and *CCDC40* mutations [Becker-Heck et al., 2011; Merveille et al., 2011]. The patients were all diagnosed based on having a classic PCD phenotype, including recurrent respiratory tract infections, pneumonia, rhinosinusitis, otitis media usually requiring repeated grommet insertion, and age-dependent bronchiectasis, where chest CT data was available. Most patients showed symptoms in the neonatal period, with respiratory distress, as well as recurrent airway infections. The clinical details for the affected families are shown in Supp. Table S2. In addition, patients showed abnormal cilia ultrastructure and motility at the electron and light microscopic levels respectively, as described below.

Combined whole exome sequencing and Sanger sequencing analysis in the 54 families identified a total of 25 different putative mutations, 12 in *CCDC39* and 13 in *CCDC40*, that affected a total of 47 patients in 37 families (Table 1). All the changes consisted of frameshift, nonsense, and essential splice-site mutations, the latter all affecting the 100% conserved splicing consensus intronic nucleotides. None of the identified variants are present in dbSNP or the 1000 Genomes Project and NHLBI ESP Exome Variant Server exome repositories, nor where they detected in 180 exomes available via the UK10K project (uk10k.org.uk). Genotyping of all available members of the affected families carrying *CCDC39/40* mutations showed that all the identified variants segregated correctly in association with disease status, having an autosomal recessive inheritance pattern. Of the 37 families carrying *CCDC39/40* mutations, segregation was possible for 26 families, the other 11 families being represented by single affected patients (Figs. 1A and B, and Supp.

Table 1. *CCDC39* and *CCDC40* Mutations Identified in PCD Patients in this Study

Family	Origin	Cons	Method	Gene	Allele 1	Effect	Location	Allele 2	Effect	Location
UCL22	N. Europe (Germany)	Y	WES	*CCDC39*	c.1486_1487insA; p.Ser496Tyrfs15*	Frameshift	Exon 11	c.2159–2A>G; essential splice site	Splice	Intron 15
UCL31	N. Europe (UK)	N	Sanger	*CCDC39*	c.2596G>T; p.Glu866*	Nonsense	Exon 19	c.2596G>T; p.Glu866*	Nonsense	Exon 19
UCL102	N. Europe (UK)	N	WES	*CCDC39*	c.357+1G>C; essential splice site	Splice	Intron 3	c.151C>T; p.Arg51*	Nonsense	Exon 2
UCL113	N. Europe (UK)	N	Sanger	*CCDC39*	c.1795C>T; p.Arg599*	Nonsense	Exon 13	c.1795C>T; p.Arg599*	Nonsense	Exon 13
UCL186	Zimbabwe	N	WES	*CCDC39*	c.2039_2040delGT; p.Cys680Phefs9*	Frameshift	Exon 15	c.526_527delCT; p.Leu176Alafs10*	Frameshift	Exon 5
UCL206	N. Europe (UK)	N	WES	*CCDC39*	c.664G>T; p.Glu222*	Nonsense	Exon 6	c.526_527delCT; p.Leu176Alafs10*	Frameshift	Exon 5
UCL210	Afghanistan (Punjabi isolate)	N	WES	*CCDC39*	c.2245G>T; p.Glu749*	Nonsense	Exon 16	c.2245G>T; p.Glu749*	Nonsense	Exon 16
UCL211	N. Europe (Portugal)	N	WES	*CCDC39*	c.1450delA; p.Ile484Leufs47*	Frameshift	Exon 11	c.357+1G>C; essential splice site	Splice	Intron 3
UNC64	N. Europe (USA)	N	Sanger	*CCDC39*	c.830_831delCA; p.Thr277Argfs3*	Frameshift	Exon 7	c.830_831delCA; p.Thr277Argfs3*	Frameshift	Exon 7
UCL8	N. Europe (UK)	N	Sanger	*CCDC40*	c.2712–1G>T; essential splice site	Splice	Intron 16	c.2712–1G>T; essential splice site	Splice	Intron 16
UCL17	N. Europe (Belgium)	N	Sanger	*CCDC40*	c.248delC; p.Ala83Valfs84*	Frameshift	Exon 3	c.248delC; p.Ala83Valfs84*	Frameshift	Exon 3
UCL114	N. Europe (UK)	N	WES	*CCDC40*	c.2712–1G>T; essential splice site	Splice	Intron 16	c.2712–1G>T; essential splice site	Splice	Exon 17
UCL129	Pakistan	Y	Sanger	*CCDC40*	c.1415delG; p.Arg472fs3*	Frameshift	Exon 9	c.1415delG; p.Arg472fs3*	Frameshift	Exon 9
UCL133	Pakistan	Y	Sanger	*CCDC40*	c.1006C>T; p.Gln336*	Nonsense	Exon 7	c.1006C>T; p.Gln336*	Nonsense	Exon 7
UCL147	N. Europe (UK)	N	WES	*CCDC40*	c.248delC; p.Ala83Valfs84*	Frameshift	Exon 3	c.248delC; p.Ala83Valfs84*	Frameshift	Exon 3
UCL199	N. Europe (UK)	N	Sanger	*CCDC40*	c.248delC; p.Ala83Valfs84*	Frameshift	Exon 3	c.248delC; p.Ala83Valfs84*	Frameshift	Exon 3
UCL216	N. Europe (UK)	N	WES	*CCDC40*	c.248delC; p.Ala83Valfs84*	Frameshift	Exon 3	c.248delC; p.Ala83Valfs84*	Frameshift	Exon 3
OP-559	S. Europe (Turkish)	N	Sanger	*CCDC40*	c.3175C>T; p.Arg1059*	Nonsense	Exon 19	c.3175C>T; p.Arg1059*	Nonsense	Exon 19
OP-560	N. Europe (Belgian)	N	Sanger	*CCDC40*	c.248delC; p.Ala83Valfs84*	Frameshift	Exon 3	c.248delC; p.Ala83Valfs84*	Frameshift	Exon 3
OP-561	Africa (Moroccan)	Y	Sanger	*CCDC40*	c.1464delC; p.Ile488Ilefs19*	Frameshift	Exon 10	c.1464delC; p.Ile488Ilefs19*	Frameshift	Exon 10
KUL-001	N. Europe (Belgian)	N	WES	*CCDC40*	c.248delC; p.Ala83Valfs84*	Frameshift	Exon 3	c.687delA; p.Pro229Profs58*	Frameshift	Exon 5
UNC120	N. Europe (USA)	N	Sanger	*CCDC40*	c.248delC; p.Ala83Valfs84*	Frameshift	Exon 3	c.248delC; p.Ala83Valfs84*	Frameshift	Exon 3
UNC122	N. Europe (USA)	N	Sanger	*CCDC40*	c.248delC; p.Ala83Valfs84*	Frameshift	Exon 3	c.248delC; p.Ala83Valfs84*	Frameshift	Exon 3
UNC130	N. Europe (USA)	Y	Sanger	*CCDC40*	c.2440C>T; p.Arg814*	Nonsense	Exon 14	c.2440C>T; p.Arg814*	Nonsense	Exon 14
UNC175	N. Europe (USA)	N	Sanger	*CCDC40*	c.961C>T; p.Arg321*	Nonsense	Exon 7	c.3129delC; p.Asp1043Aspfs36*	Frameshift	Exon 19
UNC176	N. Europe (USA)	N	Sanger	*CCDC40*	c.248delC; p.Ala83Valfs84*	Frameshift	Exon 3	c.248delC; p.Ala83Valfs84*	Frameshift	Exon 3
UNC188	N. Europe (USA)	N	Sanger	*CCDC40*	c.248delC; p.Ala83Valfs84*	Frameshift	Exon 3	c.248delC; p.Ala83Valfs84*	Frameshift	Exon 3
UNC281	N. Europe (USA)	N	Sanger	*CCDC40*	c.248delC; p.Ala83Valfs84*	Frameshift	Exon 3	c.248delC; p.Ala83Valfs84*	Frameshift	Exon 3
UNC299	N. Europe (USA)	N	Sanger	*CCDC40*	c.940–2A>G; essential splice site	Splice	Intron 6	c.344delC; p.Pro115Argfs52*	Frameshift	Exon 3
UNC336	N. Europe (USA)	N	Sanger	*CCDC40*	c.248delC; p.Ala83Valfs84*	Frameshift	Exon 3	c.248delC; p.Ala83Valfs84*	Frameshift	Exon 3
UNC337	N. Europe (USA)	N	Sanger	*CCDC40*	c.248delC; p.Ala83Valfs84*	Frameshift	Exon 3	c.248delC; p.Ala83Valfs84*	Frameshift	Exon 3
UNC455	N. Europe (USA)	N	Sanger	*CCDC40*	c.248delC; p.Ala83Valfs84*	Frameshift	Exon 3	c.248delC; p.Ala83Valfs84*	Frameshift	Exon 3
UNC507	N. Europe (USA)	N	Sanger	*CCDC40*	c.248delC; p.Ala83Valfs84*	Frameshift	Exon 3	c.248delC; p.Ala83Valfs84*	Frameshift	Exon 3
UNC533	N. Europe (USA)	N	Sanger	*CCDC40*	c.248delC; p.Ala83Valfs84*	Frameshift	Exon 3	c.961C>T; p.Arg321*	Nonsense	Exon 7
UNC553	N. Europe (USA)	N	Sanger	*CCDC40*	c.248delC; p.Ala83Valfs84*	Frameshift	Exon 3	c.248delC; p.Ala83Valfs84*	Frameshift	Exon 3
UNC609	N. Europe (USA)	N	Sanger	*CCDC40*	c.248delC; p.Ala83Valfs84*	Frameshift	Exon 3	c.248delC; p.Ala83Valfs84*	Frameshift	Exon 3
UNC660	N. Europe (USA)	N	Sanger	*CCDC40*	c.1345C>T; p.Arg449*	Nonsense	Exon 9	c.2712–1G>T; essential splice site	Splice	Intron 16

Nucleotide numbering reflects cDNA, +1 corresponds to the A of the ATG translation initiation codon in the reference sequences for *CCDC39* (NM_181426.1) and *CCDC40* (NM_017950.2), according to journal guidelines (www.hgvs.org/mutnomen). The initiation codon is codon 1.

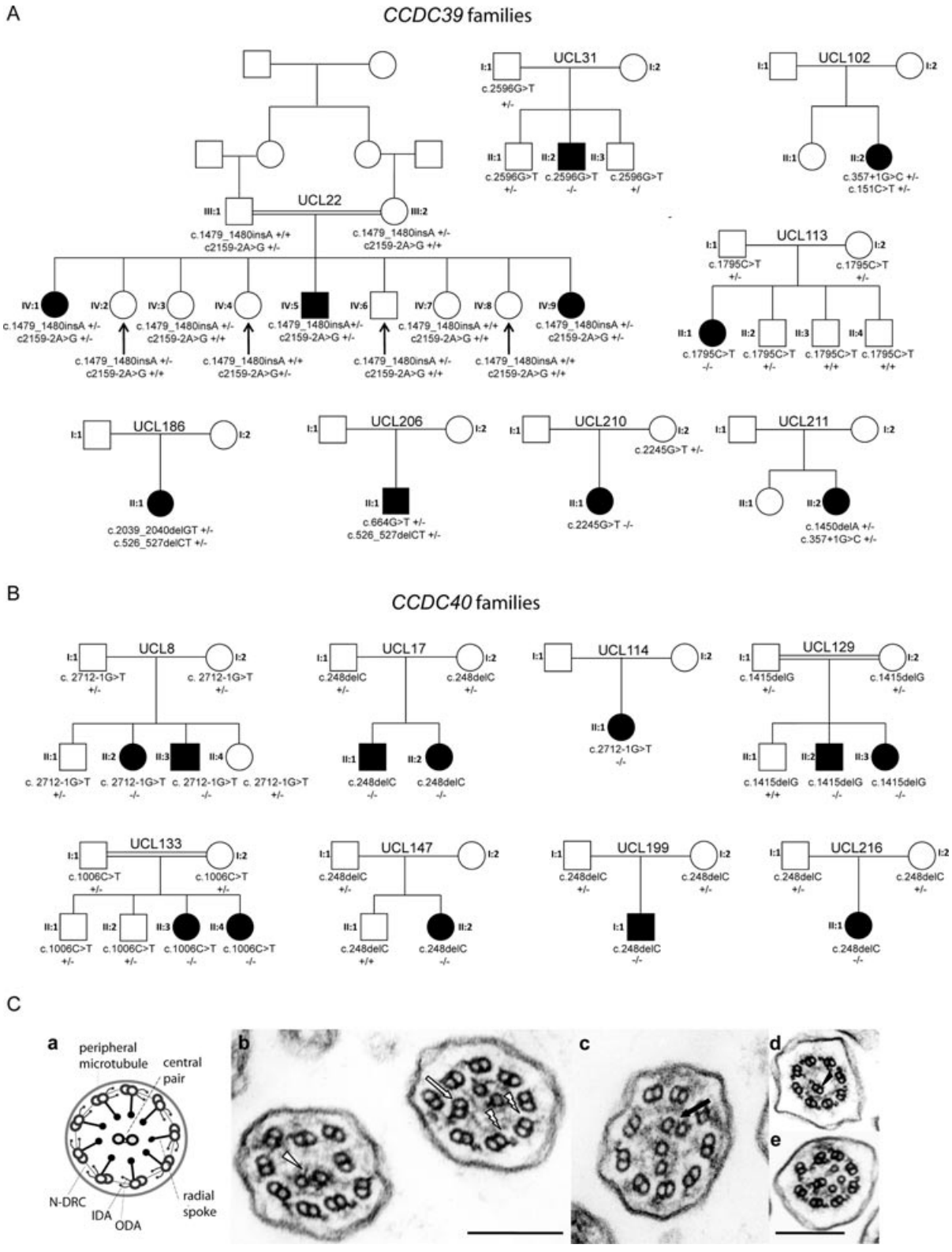

Figure 1. Mutation segregation and ultrastructural defects in selected *CCDC39* and *CCDC40* patients. **A and B:** PCD family pedigrees from the UCL-ICH cohort with autosomal recessive inheritance of *CCDC39* and *CCDC40* mutations. Affected individuals are indicated by black symbols, consanguineous marriages by a double horizontal line. Segregation patterns for the rest of the cohort are shown in Supp. Figure S1. **C:** (**a**) Normal 9+2 ciliary ultrastructure shown; ODA, outer dynein arm; IDA, inner dynein arm; N-DRC, nexin–dynein regulatory complex. Representative transmission electron micrographs of cells from nasal brush biopsy of *CCDC40* patient UCL114 II:1 show (**b**) consistent loss of inner dynein arms (lightening strikes), typical translocation to the centre of peripheral outer doublet microtubules (white arrow), accentric microtubular central pairs (white arrow head). In addition both extra central microtubules (**c**, black arrow) and total absence of the central microtubular pair (**d**, black arrowhead) were occasionally seen. (**e**) Similar findings were observed in a fallopian tube biopsy of the same patient. Scale bar, 200 nm.

Fig. S1). Thus, in this study just 17/54 families did not carry *CCDC39* and *CCDC40* variants, so these two genes accounted for 69% (37/54) of families.

In all patients with either *CCDC39* or *CCDC40* mutations, TEM of respiratory bronchial epithelial cells showed similar microtubule disorganization comprising disorganization of the peripheral microtubule doublets, absent or shifted central pairs. In all samples, there was a documented reduction or complete loss of the IDAs. Therefore, the *CCDC39* and *CCDC40* mutations cause defects that are indistinguishable by TEM.

A detailed clinical review was performed for six *CCDC39* and three *CCDC40* patients under the care of the Royal Brompton Hospital London that were part of the UCL-ICH cohort, then compared with findings on the UNC cohort of 20 patients. Their nasal nitric oxide levels were low in both cohorts at 45–79 ppb and 6–34 nl/min respectively, as expected for PCD patients where the normal mean level is 639 ppb (range 422–890) [Shoemark and Wilson, 2009]. TEM of at least 30 cilia cross-sections was examined in UCL-ICH patients, which revealed disarrangement of the outer microtubular doublets in 43% (*CCDC39*) and 36% (*CCDC40*) of cilia cross-sections, mainly involving translocation of peripheral microtubular doublets and acentric microtubular central pairs (Fig. 1C(b)–(d)). Other less prominent features included additional central microtubules or absence of the central pair structures (Fig. 1C(c)–(e)). IDAs were absent from 69% (*CCDC39*) and 90% (*CCDC40*) of cilia cross-sections (Fig 1C(b)–(e)). The ODA was apparent throughout. In one subject with *CCDC40* mutations, a fallopian tube biopsy revealed similar abnormalities (Fig. 1C(e)). The UNC study found similar results in TEM of at least 30 cilia cross-sections from *CCDC39/40* patients, with 26% of cilia on average showing microtubule disorganization and 92% showing IDAs lost on average, and ODAs present in all.

High speed video analysis of ciliated nasal brush biopsies of UCL-ICH patients with *CCDC39* mutations showed the majority of cilia to be static at 37°C (∼75%), and also at 25°C in UNC *CCDC39/40* patients. In patches where movement was present, the *CCDC39* mutant cilia beat pattern was typically stiff, rigid, and ineffective (Supp. Movies S1 and S2). This was indistinguishable from *CCDC40* (Supp. Movie S3). A control sample is shown in Supp. Movie S4. In cilia which demonstrated motility, there were a wide range of ciliary beat frequencies (range 3.3–13.0 Hz). Mean 37°C CBF was 8.1 Hz in *CCDC39* patients and 9.2 Hz in *CCDC40* patients, where the normal range is 11–16 Hz. In UNC *CCDC39/40* patients, the mean 25°C CBF was reduced to 4.3 Hz from the normal mean value of 7.3 Hz. In three *CCDC39* and one *CCDC40* patients, sperm dysmotility was also recorded (data not shown).

We used a number of protein modeling tools to identify the location of CCDC39 and CCDC40 mutations identified in this study, and those previously published, in relation to putative protein functional domains. CCDC39 has 941 residues and 10 predicted coiled-coils, in agreement with previous structural modeling [Merveille et al., 2011], and CCDC40 has 1,142 residues and eight predicted coiled-coils (Figs. 2A and B). Both proteins contain two large structural maintenance of chromosomes (SMC) conserved domains, which, as previously discussed, are found in several ciliary proteins and likely play a role in microtubule-based ciliary transport processes [Merveille et al., 2011]. A conserved BRE1 domain [Kim et al., 2005] was identified in CCDC40, but the significance is not clear. STRING predicted interactions between CCDC39 and protein phosphatase 1 F-actin cytoskeleton targeting subunit (phostensin), an actin filament-binding protein that can modulate actin dynamics that has not been connected with cilia functions [Lai et al., 2009]; and also between CCDC40 and MCTP1, a membrane protein with putative calcium-mediated signaling functions [Shin et al., 2005].

Of the 25 mutations reported here, 19 are novel to this study. Figure 2 shows the location of the identified mutations in both genes and encoded CCDC39 and CCDC40 proteins. All the identified mutations predict premature protein truncation via nonsense (5/12 and 5/13 for *CCDC39* and *CCDC40*, respectively) and frameshift effects, the latter either arising from small indels within the coding sequence (5/12 and 6/13, respectively), or from single base substitutions of the essential splice-site residues at the immediate exon–intron boundaries (2/12 and 2/13, respectively). All these variants are likely to give rise to null alleles via nonsense-mediated decay, indicating that the IDA and microtubule disorganization phenotype arises from complete loss of these proteins and consequent loss-of-function. This supports the published evidence that mutations in *CCDC39* and *CCDC40* have a similar functional effect in being highly deleterious [Becker-Heck et al., 2011; Merveille et al., 2011]. No particular clustering of mutations is evident because in both proteins, the changes that we have identified, and previously published mutations, are evenly distributed across the gene and protein structure. This suggests that protein termination at any point leads to the same deleterious dysfunction.

This study identified six mutations that have already been reported: a *CCDC39* splice-site mutation c.357+1G>C [Merveille et al., 2011] and the *CCDC40* frameshift mutations c.248delC and c.3129delC; and nonsense mutations c.2440C>T, c.961C>T, and c.1345C>T [Becker-Heck et al., 2011; Nakhleh et al., 2012]. All of these mutations are only present in patients from families of Northern European descent, except for *CCDC39* c.357+1G>C, which was reported in one Turkish and three Northern European families previously. In addition, two mutations that are novel to this study were shared amongst different families within our cohort: a *CCDC39* frameshift mutation c.526_527delCT was common to both a UK and a Zimbabwean origin family, and a *CCDC40* splice-site mutation c.2712–1G>T was shared in two UK and one US families.

We found that the *CCDC40* frameshift mutation c.248delC is extremely common, and is restricted to families of N. European origin spread worldwide, suggesting an ancient shared ancestry and past Founder effect mutation occurrence. c.248delC accounts for 34/56 N. European ancestry disease chromosomes in CCDC40 disease, a remarkable 63% (Table 1). It is not known whether the other smaller putative "hotspot" mutations may also represent Caucasian N. European-origin founder effect mutations, or whether they are functionally significant changes that have occurred separately many times in different countries. Despite the fact that only five out of the total 37 *CCDC39/40* families carrying mutations were consanguineous, there was an overall predominance of homozygous changes amongst the families, with 27/37 (73%) of *CCDC39/40* families carrying homozygous changes due to the identical alleles being inherited from both parents. The Turkish origin in one family for *CCDC39* c.357+1G>C [Merveille et al., 2011] and Zimbabwean origin in one family for *CCDC39* c.526_527delCT may indicate a more complex evolution of these common mutations than a N. European founder effect, and the possibility of nonfounder mutation hotspots. However, firm conclusions are precluded by the small family numbers. It should be noted that although the family UCL210 carrying a homozygous nonsense mutation in *CCDC40*, c.2245G>T, was not aware of familial consanguinity, they orginate from a small Punjabi-speaking isolate located in Afghanistan likely to have underlying ancestral endogamy and consanguinity.

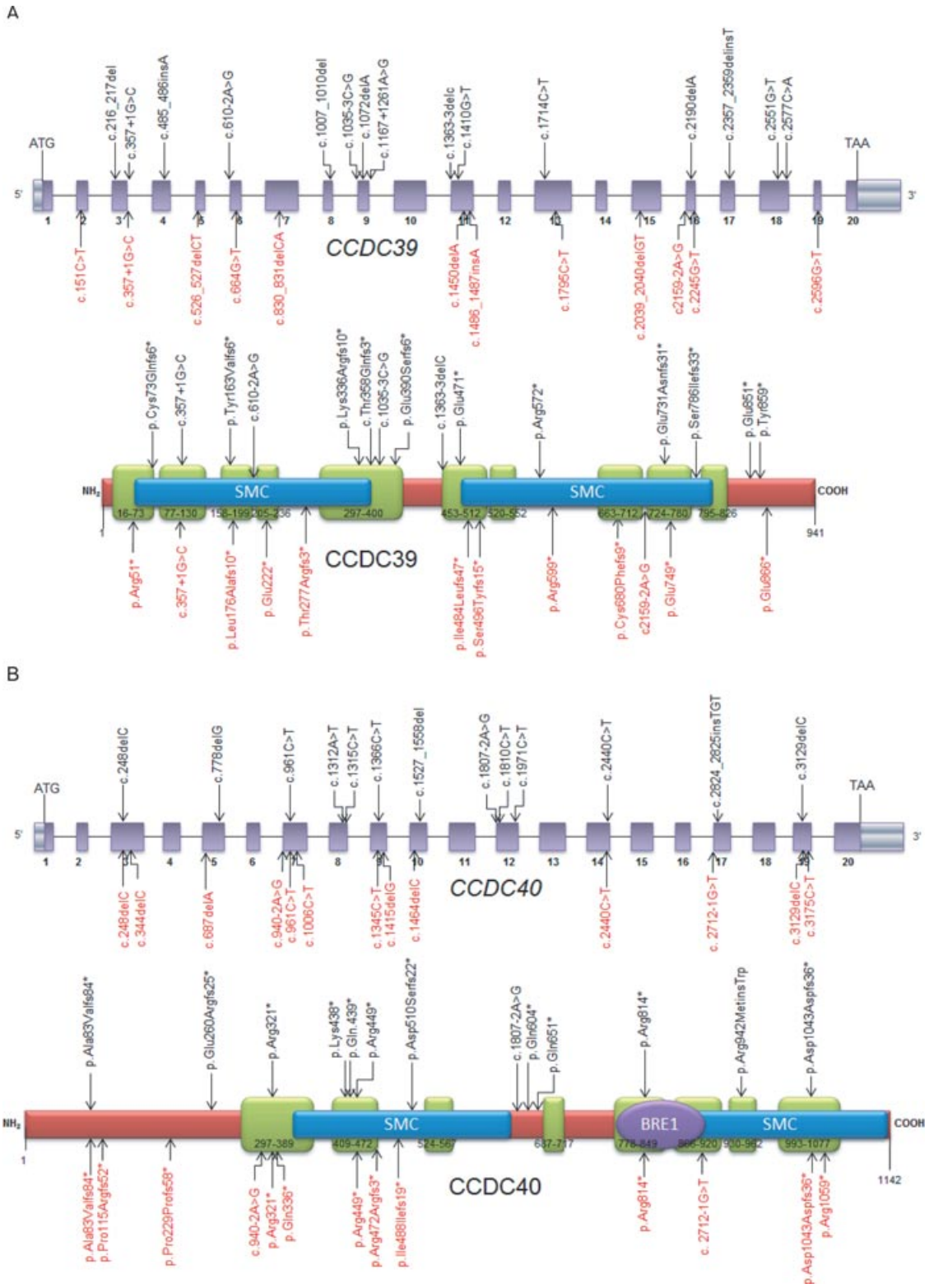

Figure 2. Location of mutations in *CCDC39* and *CCDC40*. **A and B:** Location of *CCDC39* and *CCDC40* mutations identified in this study indicated below the gene and protein images in red; mutations identified in three previous studies indicated above in black [Becker-Heck et al., 2011; Merveille et al., 2011; Nakhleh et al., 2012]. Several predicted protein domains are indicated by rectangles: coiled coil domains (green, amino acid numbers shown), structural maintenance of chromosomes domains (SMC, blue) and domains with similarity to yeast BRE1 histone ubiquitylation protein (BRE1, purple).

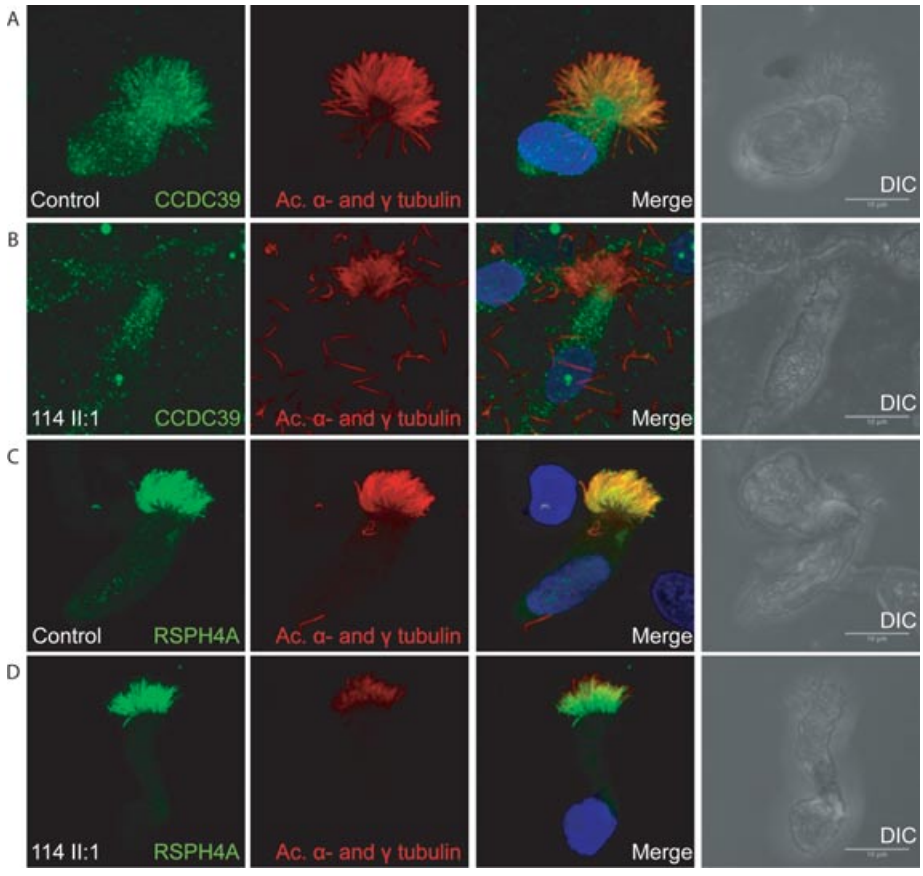

Figure 3. Localization of axonemal components in *CCDC40* patient respiratory cells. **A:** Representative immunofluorescent images of respiratory cells localize CCDC39 protein (green) along the length of the ciliary axonemes in control cells. **B:** Complete absence of CCDC39 from axonemes from a patient UCL114 II:1 carrying *CCDC40* mutations. Dual staining with antiacetylated alpha tubulin (axonemes) and antigamma tubulin (basal bodies) was used to stain the cilia (red). **C and D:** RSPH4A (green) localizes along the length of axonemes at similar levels in cells from both control and patient UCL114 II:1 carrying *CCDC40* mutations. DNA in nuclei was stained using DAPI. DIC indicates differential interference contrast microscopy Scale bar, 10 μm images.

The ciliary ultrastructure of patients with *CCDC39* and *CCDC40* mutations has been referred to as "radial spoke defect," and several reports have suggested that radial spokes are defective [Antonelli et al., 1981; Becker-Heck et al., 2011; Merveille et al., 2011; Sturgess et al., 1979]. We sought to investigate radial spoke structures in the patients at the molecular level, by high-resolution immunofluorescence analysis of nasal epithelial cells. In one *CCDC40* mutation patient UCL114 II:1, we confirmed an absence of the CCDC39 protein along the length of the axoneme in all cilia analyzed in this patient (Figs. 3A and B). These findings are consistent with published information reporting the loss of CCDC39 from axonemes of CCDC40 mutant cilia. However, both RSPH4A, which is a radial spoke "head" component [Yang et al., 2006], and ROPN1L/RSP11, which is a radial spoke "stalk" component [O'Toole et al., 2012; Yang et al., 2006] were present in axonemes from the patient as well as controls, with no differences in protein levels observable (Figs. 3C and D, and Supp. Fig. S2). This shows for the first time that components of the radial spoke structures are present in axonemes of patients that have long been typically referred to as "radial spoke defect." These data do not however prove that these radial spoke proteins are properly localized in the cilia superstructure, thus, they may be present but not functioning correctly.

Discussion

This study shows that *CCDC39* and *CCDC40* mutations are the major cause of PCD in patients with the previously termed `radial spoke defect," which is characterized by a ciliary axonemal loss of IDAs and axonemal disorganization. We report the identification of 25 different allelic mutations in *CCDC39* and *CCDC40* affecting a total of 46 PCD patients in 37 families. Nineteen of the mutations are novel to this study, whereas six are shared with patients in three previously published reports [Becker-Heck et al., 2011; Merveille et al., 2011;Nakhleh et al., 2012]. A report of additional mutations not referred to here was also published during preparation of this manuscript [Blanchon et al., 2012]. In our cohort, two of the novel mutations are found in more than one family across different population origins. Therefore, in our patients and also in those reported elsewhere, there are putative common or "hotspot" mutations for both genes; specifically c.357+1G>C and c.526_527delCT in *CCDC39*, and c.248delC, c.3129delC, c.2440C>T, c.961C>T, c.1345C>T, and c.2712–1G>T in *CCDC40*. The c.248delC mutation is very common, affecting 18/28 *CCDC40* families (64%) in this study, in particular US-origin families. The total number of different alleles in *CCDC39/40* is smaller than might be expected from the outbred populations we have analyzed. This collective

evidence is rather unusual for PCD disease and supports the idea that critical regions or important functional residues within the two proteins may be repeatedly vulnerable to mutation arising separately within different populations, probably combined with some localized founder effects.

Mutations in either gene give rise to the same ciliary and clinical phenotypes, and ciliary defects that are indistinguishable using current methodologies of TEM and high-speed video microscopy. Our TEM and cilia dysmotility findings are consistent with published findings for *CCDC39* and *CCDC40* mutation [Becker-Heck et al., 2011; Merveille et al., 2011]. Therefore, mutations in these genes give rise to analogous defects, which is consistent with similarities in their protein architecture, axonemal localization, and putative biological role(s). The large number of patients within the "radial spoke defect" subtype of PCD that carry mutations in *CCDC39/40* is striking given the extensive underlying genetic heterogeneity in PCD.

Notably, all *CCDC39/40* mutations give rise to null alleles because of nonsense, frameshift, or conserved splice-site effects. This suggests that complete loss of protein is required to give the characteristic ultrastructural defects, and individuals carrying "milder" effect alleles would likely not express a PCD-like disease phenotype, although this might affect disease severity of other airway diseases. This is in direct contrast with other ciliopathy disorders (affecting nonmotile primary cilia) where missense mutations predominantly confer disease, and it is reported that two null alleles are never seen in patients because they affect development so severely that they are incompatible with embryonic survival [Beales et al., 2007; Dagoneau et al., 2009; Davis et al., 2011. An intriguing alternative hypothesis is that *CCDC39/40* missense mutations are not observed because they may be more deleterious than loss of function mutations, rather than less deleterious, and are thus selected against in the surviving clinical patient population. This model is also plausible, for example, if CCDC39/CCDC40 were to orchestrate cilia assembly in multiprotein complexes, such that loss of function mutations could be better tolerated than gain-of-function missense mutations.

Combining our data with that of the three previous reports, a total of 26 mutations in *CCDC39* and 21 mutations in *CCDC40* have been identified, all encoding predicted null alleles. In N-DRC *Chlamydomonas* null-mutant strains, loss of any one of the N-DRC components gives rise to complete loss of the entire N-DRC structure [Piperno et al., 1994]. *CCDC39* and *CCDC40* mutation patients also lack at least some of the N-DRC structure, and this also appears to be associated with mutations causing complete loss of protein.

The predicted loss-of-function reported for all *CCDC39* and *CCDC40* mutations correlates with the widespread distribution of mutations across both genes, without any evidence of clustering. We expect that all mutations identified in these two genes would make the protein subject to nonsense-mediated decay; however, both proteins contain multiple functionally important domains that are highly evolutionarily conserved across species and likely critical to function. The possible role of the BRE1 domain in CCDC40 is less clear, but the large SMC domains in both proteins are thought to be involved in microtubule transporting [Merveille et al., 2011]. Both proteins have multiple coiled-coil domains, which leads to a compositional bias of charged and hydrophobic residues containing many lysine, leucine, and glutamic acid residues, which are generally located at the "surface" of the coiled-coil domains involved in conferring solubility and interaction properties. The 10 nonsense mutations identified in this study mostly affect glutamic acid or arginine residues, mostly in coiled-coil domains; however, their codon composition makes these residues prone to nonsense mutations, rather than indicating specific functional importance at those residues. Coiled-coil domains are found in many different proteins with diverse functions [Strauss and Keller, 2008], including structural and motor proteins. They are also associated with signal transduction functions, and assembly/disassembly of protein complexes, which may relate to the IDA–N-DRC–radial spoke complexes of cilia. If the stability provided by multiple coiled-coils is mutated, this may result in reduced efficiency or loss of protein function. Alternatively, some motor proteins have intrinsic instability in the coiled-coil domains to allow the relaxing of tertiary structure and movement of the motor proteins, which could be important in the cilia.

In contrast with N-DRC components, components of the radial spokes, such as the spoke "head" protein RSPH4A and spoke "stalk" protein ROPN1L, are present in CCDC40 mutant axonemes. This provides the first evidence that the ultrastructural defect in patients with *CCDC39/40* mutations, commonly referred to as "radial spoke defect," may not reflect a loss of spokes, but proves supporting evidence that they may remain largely intact. We have not been able to exclude the possibility that radial spoke components may be present, but mislocalized, misattached, incomplete, or nonfunctional for other reasons. However, we can conclude that this defect may be more accurately referred to as "IDA and microtubular disorganisation defect," rather than "radial spoke defect."

It is not yet clear how this ciliary ultrastructural defect arises because little is known about the formation and coassembly of the human IDAs, radial spokes, and N-DRC structures, which are all attached in close proximity at the peripheral doublets. These components are all positioned at regular periodicity along the entire axoneme length, and form a sophisticated regulatory network governing dynein activity that is key to cilia motility. The loss of IDAs and N-DRC together in CCDC39 and CCDC40 mutant axonemes is consistent with the role that the N-DRC plays in tethering of IDA components, as shown in *Chlamydomonas.* The resultant disorganization of the peripheral microtubules and the resultant instability of the central pair apparatus, indicates that these structures are critical for integrity and motility of the axoneme. Studies of *Chlamydomonas* motility mutant strains suggest the N-DRC has a number of roles apart from binding of the IDAs to the peripheral microtubules, which include mediating signaling from the central pair–radial spoke complex to the dynein arms, and influencing dynein-controlled axonemal bending [Lin et al., 2011; Piperno et al., 1994]. Thus, a deficiency in these regulatory mechanisms could also explain the defect. In contrast, even though the radial spokes are located close to the IDA–N-DRC components of axonemes, they may not be directly involved in the dysmotility in CCDC39 and CCDC40 mutation patients, but are bystanders that are perturbed secondarily to microtubule disorganization.

In conclusion, the IDA and microtubular disorganisation defect accounts for at least 12% of PCD cases, and the great majority of these are caused by mutations in *CCDC39* and *CCDC40* (69% in this study). Mutations in these genes may have a specially increased prevalence within the isolated and consanguineous Afghanistan-Punjabi and UK-based Pakistani populations. The high prevalence of these two genes, together, as causative for this subtype of PCD, makes these results significant for clinical application, including the development of prenatal and carrier genetic tests in at-risk families, and for development of genetic therapeutic strategies.

Acknowledgments

We would like to thank all the PCD patients and families, Michele Manion and the U.S. PCD Foundation, Fiona Copeland, and the U.K. PCD Family Support Group. We thank Angelina Heer, Carmen Kopp, Denise Nergenau, and Karin Sutter for excellent technical assistance.. We thank Drs. John

Carson, Milan Hazucha, Hilda Metjian, Stephanie Davis, Ms. Susan Minnix, Ms. Kimberly Burns, Peter Noone, Christine Olson, and Lu Huang from UNC Chapel Hill; Consortium PIs, Drs. Sharon Dell, Carlos Milla, and Ken Olivier, and all the coordinators for the "Genetics Disorders of Mucociliary Clearance Consortium (GDMCC) that is part of the Rare Disease Clinical Research Network (http://rarediseasenetwork.epi.usf.edu/gdmcc/index.htm). We thank Robert Mueller, Yannick Crow, Astrid Weber, Maggie Meeks, Rahul Chodhari, and R. Mark Gardiner for patient recruitment and their involvement in the project. We thank Mellisa Dixon and Sarah Donovan for electron and light microscopy at Royal Brompton Hospital. These contents are solely the responsibility of the authors and do not necessarily represent the official view of NCRR or NIH. We thank all the participants of the UK10K RARE group, as listed in the Supporting Information file, that is part of the UK10K Consortium (uk10k.org.uk) in particular Matthew Hurles, Saeed Al Turki, and Philip Beales.

Disclosure statement: The authors declare no conflict of interest.

References

1000 Genomes Project Consortium. 2010. A map of human genome variation from population-scale sequencing. Nature 467:1061–1073.

Adzhubei IA, Schmidt S, Peshkin L, Ramensky VE, Gerasimova A, Bork P, Kondrashov AS, Sunyaev SR. 2010. A method and server for predicting damaging missense mutations. Nat Methods 7:248–249.

Altschul SF, Madden TL, Schaffer AA, Zhang J, Zhang Z, Miller W, Lipman DJ. 1997. Gapped BLAST and PSI-BLAST: a new generation of protein database search programs. Nucleic Acids Res 25:3389–3402.

Antonelli M, Modesti A, De AM, Marcolini P, Lucarelli N, Crifo S. 1981. Immotile cilia syndrome: radial spokes deficiency in a patient with Kartagener's triad. Acta Paediatr Scand 70:571–573.

Bartoloni L, Blouin JL, Pan Y, Gehrig C, Maiti AK, Scamuffa N, Rossier C, Jorissen M, Armengot M, Meeks M, Mitchison HM, Chung EM, DeLozier-Blanchet CD, Craigen WJ, Antonarakis SE. 2002. Mutations in the DNAH11 (axonemal heavy chain dynein type 11) gene cause one form of situs inversus totalis and most likely primary ciliary dyskinesia. Proc Natl Acad Sci USA 99:10282–10286.

Beales PL, Bland E, Tobin JL, Bacchelli C, Tuysuz B, Hill J, Rix S, Pearson CG, Kai M, Hartley J, Johnson C, Irving M, Elcioglu N, Winey M, Tada M, Scambler PJ. 2007. IFT80, which encodes a conserved intraflagellar transport protein, is mutated in Jeune asphyxiating thoracic dystrophy. Nat Genet 39:727–729.

Becker-Heck A, Loges NT, Omran H. 2012. Dynein dysfunction as a cause of primary ciliary dyskinesia and other ciliopathies. In: King SM, editor. Dyneins. Waltham, MA: Academic Press, Elsevier. p 602–628.

Becker-Heck A, Zohn IE, Okabe N, Pollock A, Lenhart KB, Sullivan-Brown J, McSheene J, Loges NT, Olbrich H, Haeffner K, Fliegauf M, Horvath J, et al. 2011. The coiled-coil domain containing protein CCDC40 is essential for motile cilia function and left-right axis formation. Nat Genet 43:79–84.

Blanchon S, Legendre M, Copin B, Duquesnoy P, Montantin G, Kott E, Dastot F, Jeanson L, Cachanado M, Rousseau A, Papon JF, Beydon N, et al. 2012. Delineation of CCDC39/CCDC40 mutation spectrum and associated phenotypes in primary ciliary dyskinesia. J Med Genet 49:410–416.

Castleman VH, Romio L, Chodhari R, Hirst RA, de Castro SC, Parker KA, Ybot-Gonzalez P, Emes RD, Wilson SW, Wallis C, Johnson CA, Herrera RJ, et al. 2009. Mutations in radial spoke head protein genes RSPH9 and RSPH4A cause primary ciliary dyskinesia with central-microtubular-pair abnormalities. Am J Hum Genet 84:197–209.

Chilvers MA, Rutman A, O'Callaghan C. 2003. Ciliary beat pattern is associated with specific ultrastructural defects in primary ciliary dyskinesia. J Allergy Clin Immunol 112:518–524.

Dagoneau N, Goulet M, Genevieve D, Sznajer Y, Martinovic J, Smithson S, Huber C, Baujat G, Flori E, Tecco L, Cavalcanti D, Delezoide AL, et al. 2009. DYNC2H1 mutations cause asphyxiating thoracic dystrophy and short rib-polydactyly syndrome, type III. Am J Hum Genet 84:706–711.

Davis EE, Zhang Q, Liu Q, Diplas BH, Davey LM, Hartley J, Stoetzel C, Szymanska K, Ramaswami G, Logan CV, Muzny DM, Young AC, et al. 2011. TTC21B contributes both causal and modifying alleles across the ciliopathy spectrum. Nat Genet 43:189–196.

Duquesnoy P, Escudier E, Vincensini L, Freshour J, Bridoux AM, Coste A, Deschildre A, de BJ, Legendre M, Montantin G, Tenreiro H, Vojtek AM, et al. 2009. Loss-of-function mutations in the human ortholog of Chlamydomonas reinhardtii ODA7 disrupt dynein arm assembly and cause primary ciliary dyskinesia. Am J Hum Genet 85:890–896.

Duriez B, Duquesnoy P, Escudier E, Bridoux AM, Escalier D, Rayet I, Marcos E, Vojtek AM, Bercher JF, Amselem S. 2007. A common variant in combination with a nonsense mutation in a member of the thioredoxin family causes primary ciliary dyskinesia. Proc Natl Acad Sci USA 104:3336–3341.

Fliegauf M, Benzing T, Omran H. 2007. When cilia go bad: cilia defects and ciliopathies. Nat Rev Mol Cell Biol 8:880–893.

Heuser T, Raytchev M, Krell J, Porter ME, Nicastro D. 2009. The dynein regulatory complex is the nexin link and a major regulatory node in cilia and flagella. J Cell Biol 187:921–933

Horani A, Druley TE, Zariwala MA, Patel AC, Levinson BT, Van Arendonk LG, Thornton KC, Giacalone JC, Albee AJ, Wilson KS, Turner EH, Nickerson DA, et al. 2012. Whole-exome capture and sequencing identifies HEATR2 mutation as a cause of primary ciliary dyskinesia. Am J Hum Genet 91:685–693.

Kim J, Hake SB, Roeder RG. 2005. The human homolog of yeast BRE1 functions as a transcriptional coactivator through direct activator interactions. Mol Cell 20:759–770.

Kispert A, Petry M, Olbrich H, Volz A, Ketelsen UP, Horvath J, Melkaoui R, Omran H, Zariwala M, Noone PG, Knowles M. 2003. Genotype-phenotype correlations in PCD patients carrying DNAH5 mutations. Thorax 58:552–554.

Knowles MR, Leigh MW, Carson JL, Davis SD, Dell SD, Ferkol TW, Olivier KN, Sagel SD, Rosenfeld M, Burns KA, Minnix SL, Armstrong MC, et al. 2012. Mutations of DNAH11 in patients with primary ciliary dyskinesia with normal ciliary ultrastructure. Thorax 67:433–441.

Knowles MR, Leigh MW, Ostrowski LE, Huang L, Carson JL, Hazucha MJ, Yin W, Berg JS, Davis SD, Dell SD, Ferkol TW, Rosenfeld M, et al. in press. Exome sequencing identifies mutations in CCDC114 as a cause of primary ciliary dyskinesia. Am J Hum Genet. 2012 Dec 19. doi:pii: S0002-9297(12)00585-X. 10.1016/j.ajhg.2012.11.003. [Epub ahead of print]

Kott E, Duquesnoy P, Copin B, Legendre M, Dastot-Le Moal F, Montantin G, Jeanson L, Tamalet A, Papon JF, Siffroi JP, Rives N, Mitchell V, et al. 2012. Loss-of-function mutations in LRRC6, a gene essential for proper axonemal assembly of inner and outer dynein arms, cause primary ciliary dyskinesia. Am J Hum Genet 91:958–964.

Konradova V, Vavrova V, Hlouskova Z, Copova M, Tomanek A, Houstek J. 1982. Ultrastructure of bronchial epithelium in children with chronic or recurrent respiratory diseases. Eur J Respir Dis 63:516–525.

Lai NS, Wang TF, Wang SL, Chen CY, Yen JY, Huang HL, Li C, Huang KY, Liu SQ, Lin TH, Huang HB. 2009. Phostensin caps to the pointed end of actin filaments and modulates actin dynamics. Biochem Biophys Res Commun 387:676–681.

Letunic I, Doerks T, Bork P. 2012. SMART 7: recent updates to the protein domain annotation resource. Nucleic Acids Res 40:D302–D305.

Li H, Durbin R. 2010. Fast and accurate long-read alignment with Burrows–Wheeler transform. Bioinformatics 26:589–595.

Lin J, Tritschler D, Song K, Barber CF, Cobb JS, Porter ME, Nicastro D. 2011. Building blocks of the nexin-dynein regulatory complex in Chlamydomonas flagella. J Biol Chem 286:29175–29191.

Loges NT, Olbrich H, Becker-Heck A, Haffner K, Heer A, Reinhard C, Schmidts M, Kispert A, Zariwala MA, Leigh MW, Knowles MR, Zentgraf H, et al. 2009. Deletions and point mutations of LRRC50 cause primary ciliary dyskinesia due to dynein arm defects. Am J Hum Genet 85:883–889.

Loges NT, Olbrich H, Fenske L, Mussaffi H, Horvath J, Fliegauf M, Kuhl H, Baktai G, Peterffy E, Chodhari R, Chung EM, Rutman A, et al. 2008. DNAI2 mutations cause primary ciliary dyskinesia with defects in the outer dynein arm. Am J Hum Genet 83:547–558.

Marchler-Bauer A, Lu S, Anderson JB, Chitsaz F, Derbyshire MK, DeWeese-Scott C, Fong JH, Geer LY, Geer RC, Gonzales NR, Gwadz M, Hurwitz DI, et al. 2011. CDD: a Conserved Domain Database for the functional annotation of proteins. Nucleic Acids Res 39:D225–D229.

Mazor M, Alkrinawi S, Chalifa-Caspi V, Manor E, Sheffield VC, Aviram M, Parvari R. 2011. Primary ciliary dyskinesia caused by homozygous mutation in DNAL1, encoding dynein light chain 1. Am J Hum Genet 88:599–607.

McDonnell AV, Jiang T, Keating AE, Berger B. 2006. Paircoil2: improved prediction of coiled coils from sequence. Bioinformatics 22:356–358.

McKenna A, Hanna M, Banks E, Sivachenko A, Cibulskis K, Kernytsky A, Garimella K, Altshuler D, Gabriel S, Daly M, DePristo MA. 2010. The Genome Analysis Toolkit: a MapReduce framework for analyzing next-generation DNA sequencing data. Genome Res 20:1297–1303.

Merveille AC, Davis EE, Becker-Heck A, Legendre M, Amirav I, Bataille G, Belmont J, Beydon N, Billen F, Clement A, Clercx C, Coste A, et al. 2011. CCDC39 is required for assembly of inner dynein arms and the dynein regulatory complex and for normal ciliary motility in humans and dogs. Nat Genet 43:72–78.

Mitchison HM, Schmidts M, Loges NT, Freshour J, Dritsoula A, Hirst RA, O'Callaghan C, Blau H, Al DM, Olbrich H, Beales PL, Yagi T, et al. 2012. Mutations in axonemal dynein assembly factor DNAAF3 cause primary ciliary dyskinesia. Nat Genet 44:381–382.

Mitchison TJ, Mitchison HM. 2010. Cell biology: how cilia beat. Nature 463:308–309.

Nakhleh N, Francis R, Giese RA, Tian X, Li Y, Zariwala MA, Yagi H, Khalifa O, Kureshi S, Chatterjee B, Sabol SL, Swisher M, et al. 2012. High prevalence of respiratory ciliary dysfunction in congenital heart disease patients with heterotaxy. Circulation 125:2232–2242.

O'Toole ET, Giddings TH, Jr., Porter ME, Ostrowski LE. 2012. Computer-assisted image analysis of human cilia and Chlamydomonas flagella reveals both similarities and differences in axoneme structure. Cytoskeleton (Hoboken) 69:577–590.

Olbrich H, Haffner K, Kispert A, Volkel A, Volz A, Sasmaz G, Reinhardt R, Hennig S, Lehrach H, Konietzko N, Zariwala M, Noone PG, et al. 2002. Mutations in DNAH5 cause primary ciliary dyskinesia and randomization of left-right asymmetry. Nat Genet 30:143–144.

Olbrich H, Schmidts M, Werner C, Onoufriadis A, Loges NT, Raidt J, Banki NF, Shoemark A, Burgoyne T, Al Turki S, Hurles ME, UK10 Consortium, et al. 2012. Recessive HYDIN mutations cause primary ciliary dyskinesia without randomization of left/right body asymmetry. Am J Hum Genet 91:672–684.

Omran H, Kobayashi D, Olbrich H, Tsukahara T, Loges NT, Hagiwara H, Zhang Q, Leblond G, O'Toole E, Hara C, Mizuno H, Kawano H, et al. 2008. Ktu/PF13 is required for cytoplasmic pre-assembly of axonemal dyneins. Nature 456:611–616.

Onoufriadis A, Paff T, Antony D, Shoemark A, Micha D, Kuyt B, Schmidts M, Petridi S, Dankert-Roelse J, Haarman E, Daniels JMA, Emes RD, et al. in press. Splice site mutations in the axonemal outer dynein arm docking complex gene CCDC114 cause primary ciliary dyskinesia. Am J Hum Genet. 2012 Dec 19. pii: S0002-9297(12)00583-6. doi: 10.1016/j.ajhg.2012.11.002. [Epub ahead of print]

Panizzi JR, Becker-Heck A, Castleman VH, Al-Mutairi DA, Liu Y, Loges NT, Pathak N, Austin-Tse C, Sheridan E, Schmidts M, Olbrich H, Werner C, et al. 2012. CCDC103 mutations cause primary ciliary dyskinesia by disrupting assembly of ciliary dynein arms. Nat Genet 44:714–719.

Papon JF, Coste A, Roudot-Thoraval F, Boucherat M, Roger G, Tamalet A, Vojtek AM, Amselem S, Escudier E. 2010. A 20-year experience of electron microscopy in the diagnosis of primary ciliary dyskinesia. Eur Respir J 35:1057–1063.

Pazour GJ. 2004. Comparative genomics: prediction of the ciliary and basal body proteome. Curr Biol 14:R575-R577.

Pennarun G, Escudier E, Chapelin C, Bridoux AM, Cacheux V, Roger G, Clement A, Goossens M, Amselem S, Duriez B. 1999. Loss-of-function mutations in a human gene related to Chlamydomonas reinhardtii dynein IC78 result in primary ciliary dyskinesia. Am J Hum Genet 65:1508–1519.

Piperno G, Mead K, LeDizet M, Moscatelli A. 1994. Mutations in the "dynein regulatory complex" alter the ATP-insensitive binding sites for inner arm dyneins in Chlamydomonas axonemes. J Cell Biol 125:1109–1117.

Rutland J, Dewar A, Cox T, Cole P. 1982. Nasal brushing for the study of ciliary ultrastructure. J Clin Pathol 35:357–359.

Schneeberger EE, McCormack J, Issenberg HJ, Schuster SR, Gerald PS. 1980. Heterogeneity of ciliary morphology in the immotile-cilia syndrome in man. J Ultrastruct Res 73:34–43.

Sherry ST, Ward MH, Kholodov M, Baker J, Phan L, Smigielski EM, Sirotkin K. 2001. dbSNP: the NCBI database of genetic variation. Nucleic Acids Res 29:308–311.

Shin OH, Han W, Wang Y, Sudhof TC. 2005. Evolutionarily conserved multiple C2 domain proteins with two transmembrane regions (MCTPs) and unusual Ca^{2+} binding properties. J Biol Chem 280:1641–1651.

Shoemark A, Dixon M, Corrin B, Dewar A. 2012. Twenty-year review of quantitative transmission electron microscopy for the diagnosis of primary ciliary dyskinesia. J Clin Pathol 65:267–271.

Shoemark A, Wilson R. 2009. Bronchial and peripheral airway nitric oxide in primary ciliary dyskinesia and bronchiectasis. Respir Med 103:700–706.

Strauss HM, Keller S. 2008. Pharmacological interference with protein–protein interactions mediated by coiled-coil motifs. Handb Exp Pharmacol:461–482.

Sturgess JM, Chao J, Wong J, Aspin N, Turner JA. 1979. Cilia with defective radial spokes: a cause of human respiratory disease. N Engl J Med 300:53–56.

Szklarczyk D, Franceschini A, Kuhn M, Simonovic M, Roth A, Minguez P, Doerks T, Stark M, Muller J, Bork P, Jensen LJ, von MC. 2011. The STRING database in 2011: functional interaction networks of proteins, globally integrated and scored. Nucleic Acids Res 39:D561-D568.

Wang K, Li M, Hakonarson H. 2010. ANNOVAR: functional annotation of genetic variants from high-throughput sequencing data. Nucleic Acids Res 38:e164.

Yang P, Diener DR, Yang C, Kohno T, Pazour GJ, Dienes JM, Agrin NS, King SM, Sale WS, Kamiya R, Rosenbaum JL, Witman GB. 2006. Radial spoke proteins of Chlamydomonas flagella. J Cell Sci 119:1165–1174.